Cytoskeletal Regulation of Mitochondrial Movements in Myoblasts

Sobia Iqbal[1,2] and David A. Hood[1,2]*

[1]School of Kinesiology and Health Science, York University, Toronto, Ontario, Canada
[2]Muscle Health Research Centre, York University, Toronto, Ontario, Canada

Mitochondria are distributed in the cell to match the energy demands, and it is their interaction with the cytoskeleton that controls their movement and displacement. Our purpose was to determine which cytoskeletal components are primarily responsible for mitochondrial movement in muscle cells. Live-cell imaging was used to visualize mitochondrial dynamics in myoblasts. Destabilization of microtubules (MT) reduced the total path length and average speed traveled by mitochondria by 64–74%, whereas actin disruption only reduced these variables by 37-40%. Downregulation of the microtubule motor proteins, Kif5B and dynein, by siRNA resulted in decreases in the average speed of mitochondrial movements, by 30 to 40%. We observed a reduction in the average speed of mitochondrial movements (by 22 to 48%) under high calcium conditions. This attenuation in the presence of calcium was negated in cells pre-treated with siRNA targeted to the microtubule motor protein adaptor, Milton, suggesting that Milton is involved in mediating mitochondrial arrest in the presence of high calcium within muscle cells. Thus, we have demonstrated that, in myoblasts, mitochondria primarily move along microtubules tracks with the aid of the motor proteins Kif5B and dynein, in a manner which is inhibited by calcium. These observations will eventually help us understand organelle movements in more complex muscle systems, such as mature myotubes subjected to elevated calcium levels and contractile activity. © 2014 Wiley Periodicals, Inc.

*Address correspondence to: David A. Hood, PhD, School of Kinesiology and Health Science, York University, Toronto, Ontario, M3J 1P3, Canada. E-mail: dhood@yorku.ca

Introduction

Mitochondria are vital organelles, critical for energy supply and cell survival. Such functional versatility is paralleled by the structural complexity of the organelle. Mitochondria can compensate for alterations in energy requirements by adjusting their size and distribution within skeletal muscle [De Vos et al., 2005]. It is their interaction with the cytoskeleton that is used to control their position, movement and anchorage within cells [Tanaka et al., 1998]. The three cytoskeletal elements, actin, microtubules and intermediate filaments act to vary the degree of scaffolding along which mitochondria are capable of moving.

The distribution of mitochondria to specific sites within the cell has consistently been linked to microtubules and actin. In neurons and cardiac myocytes, microtubules are the primary tracks governing mitochondrial movements [Morris and Hollenbeck, 1995; Yi et al., 2004], while in *Saccharomyces cerevisiae* the positioning of mitochondria is reliant on actin-based transportation [Simon et al., 1997]. Intracellular transport of cargo, such as mitochondria, to specific locations within the cytoplasm involves molecular motors that bind directly to the cargo and the cytoskeletal track. Dynein and kinesins motor proteins use microtubules to transport cargo throughout the cell. In neurons, movement along microtubules occurs either towards the cell body using cytoplasmic dynein, or away, using kinesins. There are 14 kinesin superfamilies encoded by the human and mouse genomes, consisting of more than 45 members [Hirokawa et al., 2009]. In neurons, Kinesin-1 and Kinesin-3 have been identified to regulate mitochondrial movements [Nangaku et al., 1994; Pilling et al., 2006]. Kinesin-1, also known as conventional kinesin, consists of three distinct members, Kif5A, Kif5B and Kif5C. Kif5A and Kif5C are neuron-specific, whereas Kif5B is ubiquitously expressed [Aizawa et al., 1992; Argyropoulos et al., 2009]. Inhibition of Kinesin-1 in *Drosophila* halts mitochondrial movement in motor axons [Pilling et al., 2006], and in non-neuronal cells, whereby deletion of Kif5B alters mitochondrial positioning [Tanaka et al., 1998; Wu et al., 1998]. The movement of motor proteins along

microtubules takes advantage of the dynamic instability of the tubulin polymer. Growth of microtubules allows for the continued expansion of the cytoskeleton, which motor proteins use as tracks. Conversely, the ability of microtubules to shrink is thought to be important for morphological changes in the cell, and in the reorientation of microtubules during the locomotion of organelles [Mitchison and Kirschner, 1984].

In muscle, calcium (Ca^{2+}) is a key regulator of contractile activity, but it is also an important signaling ion. Ca^{2+} has a role in the regulation of mitochondrial respiration, and it is involved in the opening of the mitochondrial permeability transition pore (mtPTP) [Crompton and Costi, 1988]. This dissipates the electrochemical proton gradient, thereby halting ATP production by oxidative phosphorylation. Calcium influx has also been found to inhibit mitochondrial movement in neurons and in cardiac myocytes [Yi et al., 2004; Macaskill et al., 2009; Wang and Schwarz, 2009]. The ability of mitochondria to respond to intracellular signals such as Ca^{2+}, is mediated by motor protein/adaptor complexes. The core of this complex is composed of the Kinesin-1 motor along with two mitochondrial-specific adaptors, mitochondrial Rho GTPase (Miro) and Milton [Wang and Schwarz, 2009]. Milton binds directly to Kinesin-1 [Smith et al., 2006], whereas Miro serves as an anchor linking Milton and Kinesin-1 to mitochondria [Glater et al., 2006]. Elevated calcium binds to the EF-hands of Miro and induces a conformational change in the protein, resulting in the dissociation of the complex from microtubules and arresting mitochondrial movements [Macaskill et al., 2009; Saotome et al., 2008; Wang and Schwarz, 2009].

It is now well-known that mitochondria are quite dynamic within certain cell types, however, how the distribution of these organelles is controlled and regulated in myoblasts has not been established. Thus, our purpose was to investigate the cytoskeletal components governing mitochondrial movements within myoblasts, and the relationship of these movements to changes in cytosolic calcium signaling. We hypothesize that microtubules and their associated motor proteins are the main cytoskeletal filament proteins involved in mitochondrial dynamics within myoblasts. Moreover, we believe that mitochondrial motility would be regulated by changes in intracellular calcium, and that adaptor proteins would be involved in the process.

Results

Microtubules are the Primary Filaments Used by Mitochondria During Trafficking

To elucidate which cytoskeletal elements are primarily responsible for mitochondrial motility within myoblasts, we disturbed microtubules and actin, and observed their effects on organelle movement. We examined the co-localization of actin (Fig. 1A) and mitochondria (Fig. 1B) in control cells (Fig. 1C), and compared them to myoblasts exposed to the actin disrupting agent cytochalasin D (Fig. 1D). Exposure to cytochalasin D resulted in the drastic rearrangement of actin filaments, such that they appeared disjoined and no longer extended throughout the length of the cell. Actin disruptions reduced the total path length and average speed of mitochondria by 37 and 40%, respectively (Figs. 1I and 1J).

Next, we then examined the effects of microtubule disruptions on mitochondrial dynamics. Cells stained with FITC-conjugated α-tubulin antibodies and treated with colchicine or taxol, displayed alterations in the structure of microtubules compared to untreated myoblasts (Figs. 1F–H). The destabilize agent, colchicine, resulted in enhanced depolymerization of microtubules (Fig. 1G). Conversely, the stabilizer, taxol is known to block microtubule disassembly. As depicted in Fig. 1H, taxol preventing normal polymerization of the filaments.

In response to depolymerization of microtubules using nocodazole and colchicine, the total path length of mitochondria was reduced by 64–72% (Fig. 1I), similar reductions were observed in the average speed traveled by the organelles (68–74%, Fig. 1J). In addition, the stabilization of microtubules by taxol also significantly altered mitochondrial motility, albeit to a lesser degree (Figs. 1I and 1J). To deduce the effects that microtubule and actin disruption would have in combination, we co-incubated myoblasts with nocodazole and cytochalasin D. Changes in mitochondrial motility were similar to the results observed with nocodazole treatment alone. We then ascertained whether disruptions in the cytoskeleton and mitochondrial movement had any effect on oxygen utilization. No significant effects on oxygen consumption were observed (Fig. 1K).

Treatment With Microtubule Disrupting Drugs Arrested Mitochondria to a Greater Extent Than Actin Depolymerization

Given the effects that cytoskeletal disruption had on mitochondrial speed, it was of interest to examine whether this reduction was due to slower movements, or to an overall greater percentage of time that mitochondria remained stationary. By transfecting mito-dsRED2 to visualize mitochondria (Fig. 2A), we determined the percentage of time that mitochondria spent in motion. To analyze the movement characteristics of individual mitochondria, kymographs were generated from the live-cell imaging videos to document the dynamic properties of the organelles. We determined that mitochondria remained in constant motion, and frequently changed their direction (Fig. 2B), as reflected by horizontal deviations in the kymograph tracings. The addition of microtubule disrupting agents reduced the motility of mitochondria, as depicted by decreased horizontal deviations in the kymograph tracings over the 5 min recording period with the addition of colchicine, nocodazole, or taxol. Interestingly, the kymograph
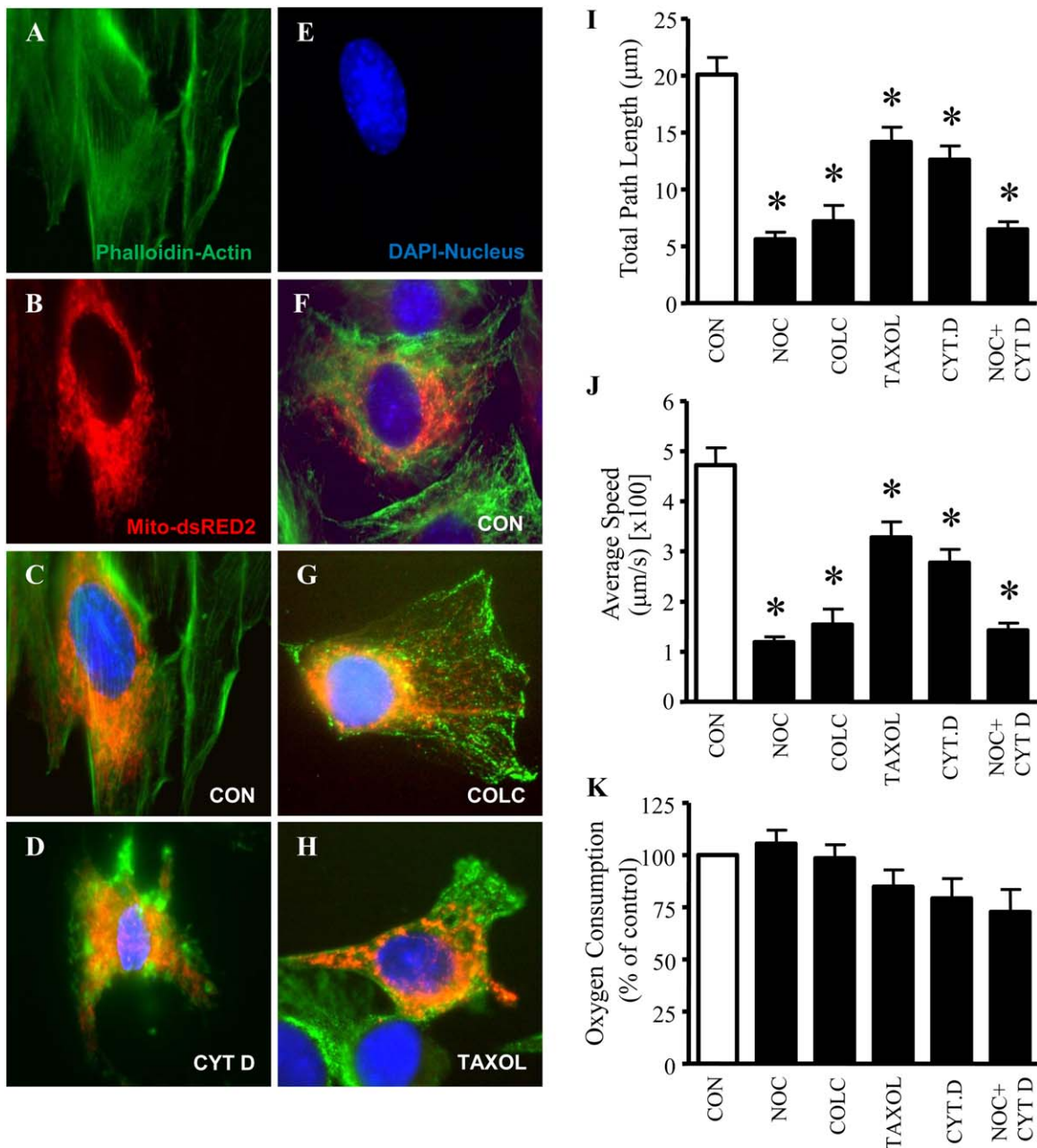
Fig. 1. Microtubules are the primary filaments used by mitochondria during trafficking. A: Myoblasts stained for actin (phalloidin, green), **B**: transfected with Mito-dsRED2 to visualize mitochondria (red), or **E**: stained with DAPI for nuclei (blue) alone. **C**: Merged images are overlays of actin (phalloidin, green), Mito-dsRED2 (mitochondria, red) and DAPI (nuclei, blue). Non-treated cells exhibited normal morphology of actin filaments. **D**: After 1 hr of treatment with cytochalasin D (CYT D), myoblasts presented cells with actin disruptions (phalloidin, green). **F**: Additionally, untreated myoblasts display normal microtubule (GFP-tubulin, green), mitochondria (Mito-dsRED2, red) and nuclei (DAPI, blue) organization. Myoblasts pre-treated with the microtubule disrupting agents. **G**: Colchicine (COLC) and **H**: TAXOL for 1 hr exhibited alterations in the microtubule structures (GFP-tubulin, green). COLC and Taxol were successful at disrupting microtubules, as indicated by the images above. **I**: Quantification of the total path length and **J**: the average speed traveled by mitochondria over the 5 min capturing time. Movement of mitochondria was determine from an average of $n = 36$–72 mitochondria from nine separate cells. **K**: Oxygen consumption was assessed in myoblasts with microtubule and/or actin disruptions using the microtubule disruptors Nocodazole (NOC), COLC, Taxol, and/or the actin disrupting agent CYT D, along with a control treatment (CON, DMSO). Values are expressed as averages ± SEM, $N = 6$. *Significantly different from CON, $P < 0.05$.

data generated from treatment with cytochalasin D was comparable to control conditions. Quantification of organelle motility revealed that alterations in microtubules increased the percentage of time that mitochondria were stopped by 1.6- to 2.7-fold (Fig. 2C). However, changes to the structure of actin filaments using by cytochalasin D treatment had no significant effect on the amount of time mitochondria were in motion in these myoblasts.
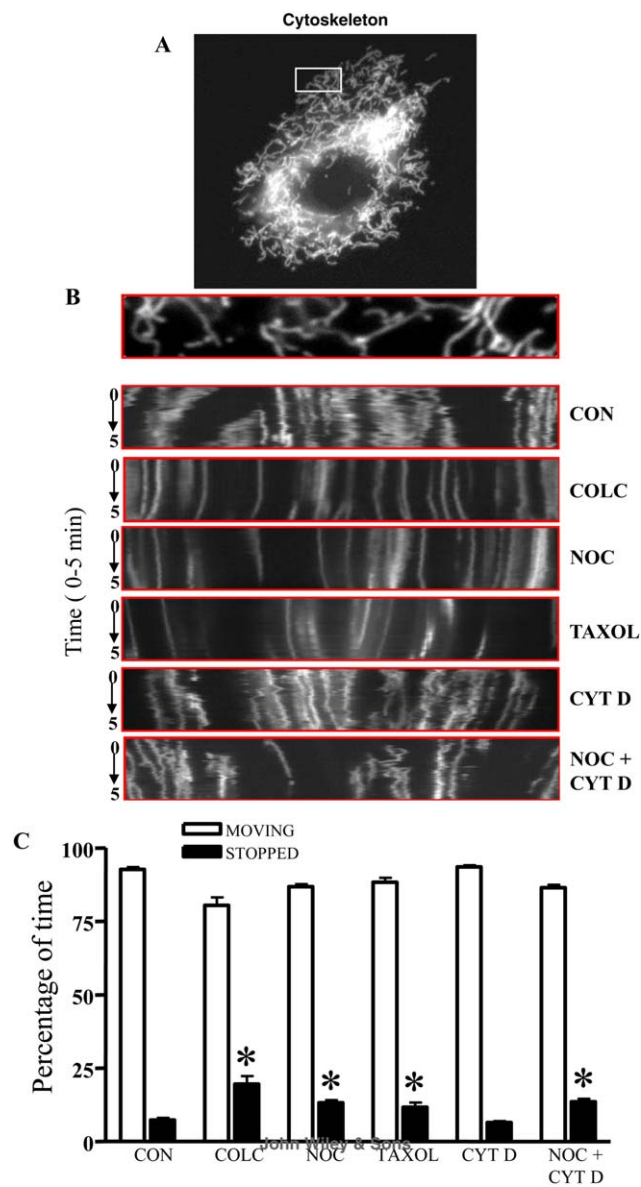
Fig. 2. Treatment with microtubule disrupting drugs arrested mitochondria to a greater extent than actin depolymerization. **A**: Mitochondrial movement in a representative myoblast transfected with mito-DsRed2. **B**: The first frame in a live-cell imaging series is displayed above with representative kymographs generated from the movies from control (CON, DMSO) Nocodazole (NOC), Colchicine (COLC), Taxol, Cytochalasin D (CYT D), or NOC + CTY D treatments. Time (0–5 min) progresses from the top to bottom in the kymograph. Whereas, the x-axis represents mitochondrial position. Vertical white lines correspond to stationary mitochondria, and horizontal deviations (vibrations from the vertical) depict moving mitochondria. **C**: The percentage of time that mitochondria spent in motion as a result of microtubule and actin disruptions was determined by monitoring the position of the organelle throughout the capturing time. Mitochondria were considered in motion if movement was greater than 0.01 μm in the 2 sec of capturing time. Movement of mitochondria was determined and averaged from n = 36–72 mitochondria from nine separate cells. Error bars represent mean $\pm$ SEM, *$P < 0.05$ vs. CON.

Knockdown of Microtubule Motor Proteins Attenuates Mitochondrial Dynamics

For mitochondria to bind to cytoskeletal elements, motor proteins are required. The transfection of siRNA probes against Kif5B and dynein in C_2C_{12} myoblasts resulted in significant reductions in their protein levels by 59 and 40%, respectively (Figs. 3A and 3B). The reduction in Kif5B was specific, and did not alter levels of mitochondrial biogenesis markers (Fig. 3A) or mitochondrial morphology proteins Mfn2, Opa1, Fis1, or Drp1 (unpublished observations). Reductions in both Kif5B and dynein resulted in similar significant decreases in the average speed of mitochondrial movements, by 30–40%, as well as in the total path length travelled by the organelles (decreased by 28–37%, Fig. 3C and 3D).

Cytosolic Calcium Regulates Mitochondrial Movement in Myoblasts

Calcium is an important signaling molecule in skeletal muscle, and as such we were interesting in examining its effects on mitochondrial motility. The Ca^{2+} ionophore, ionomycin, triggered an increase in Ca^{2+} levels that was suppressed by the addition of EGTA, as assessed by Fura2-AM ratiometric analysis (Figs. 4A and 4B). The rising phase of the cytosolic Ca^{2+} spike was accompanied by decreases in organelle motility in myoblasts (Figs. 4B and 4C). The total path length and average speed traveled by mitochondria were attenuated by 42 and 48%, respectively. The addition of EGTA permitted the recovery of mitochondrial movement, which coincided with reductions in the amount of cytosolic Ca^{2+}, (Figs. 4A–4C). Similar effects were observed with the incubation of thapsigargin, a SERCA inhibiting agent. The addition of thapsigargin significantly reduced the total path length and average speed of mitochondria by 19 and 22%, respectively (Figs. 4E and 4F). Mitochondrial motility and Ca^{2+} levels returned to resting levels with the addition of the Ca^{2+} chelator BAPTA-AM (unpublished observations).

The mechanisms by which Ca^{2+} exerts its effects are still under investigation. Milton is thought to be involved, since in neurons, Milton links mitochondria to Kif5B motor proteins, allowing mitochondria to move along microtubules in a Ca^{2+}-dependent manner [Macaskill et al., 2009; Wang and Schwarz, 2009]. Thus, we reduced the level of Milton in myoblasts and observed its influence under conditions of elevated Ca^{2+} in the presence of thapsigargin (Fig. 4G). The decrease in mitochondrial speed of movement observed with thapsigargin treatment alone was negated in cells pre-treated with Milton siRNA, suggesting that Milton is involved in mediating mitochondrial arrest in the presence of Ca^{2+}.

Discussion

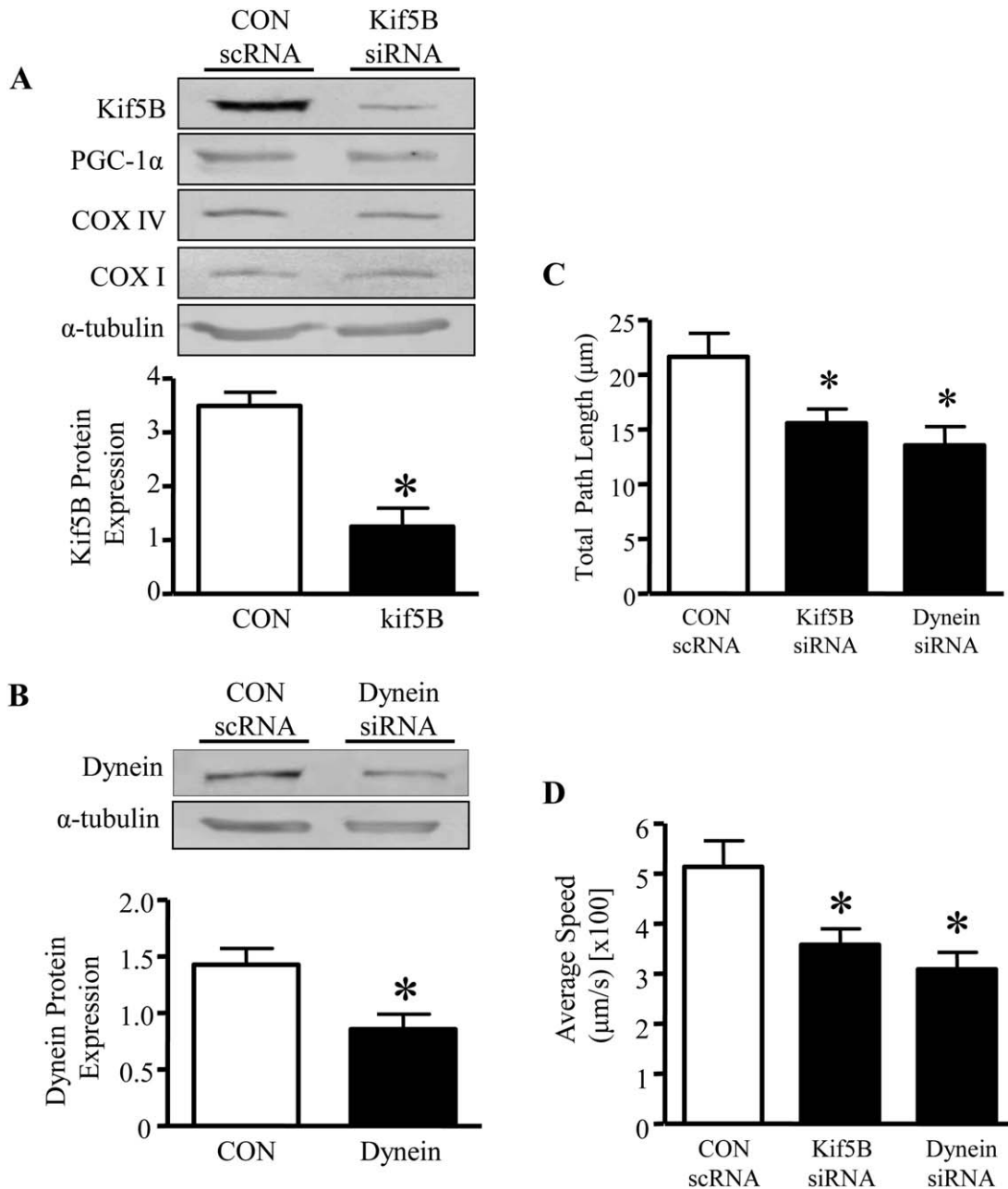In order to efficiently supply the cell with energy, mitochondria must be transported to areas of high energy

Fig. 3. Knockdown of microtubule motor proteins attenuates mitochondrial dynamics. A: Representative Western blots of markers of mitochondrial content in myoblasts treated with either scrambled control (scRNA CON) or siRNA for Kif5B (above). Quantification of protein expression of Kif5B siRNA and scRNA control (below). **B**: Representative Western blots of dynein treated with an antisense probe and its respective scRNA control (above), along with graphical quantification (below). α-tubulin was unchanged between the conditions and was used as a loading control. Experiments were repeated for five separate trials. **C**: The total path length and **D**: the average speed traveled by mitochondria was assessed in scRNA CON and siRNA treatment for Kif5B and dynein. Movement of mitochondria was averaged from $n = 20–40$ mitochondria from 5 separate cells, $*P < 0.05$ vs. CON scRNA.

demands. In neurons, mitochondria are delivered to areas where they required, and retained at sites where energy demand is high, such as growth cones, nodes of Ranvier and synapses [Fabricius et al., 1993; Morris and Hollenbeck 1993; Bindokas et al., 1998]. Within neurons, areas of high activity possess greater densities of mitochondria [King and Stocco 1996; Nguyen et al., 1997]. The movement of mitochondria to specific sites within the cell is dependent on a cytoskeleton-based transportation system. Moreover, envi-

ronmental and physiological changes are thought to influence the positioning of organelles within the cells. Thus, our purpose was to determine which cytoskeletal components were primarily responsible for mitochondrial movement within myoblasts, and to investigate the effects of calcium on mitochondrial motility. To do so, we utilized live-cell imaging techniques to monitor the dynamics of these organelles.

To address the influence of the cytoskeleton on mitochondrial motility we assessed (1) the total path length, (2)
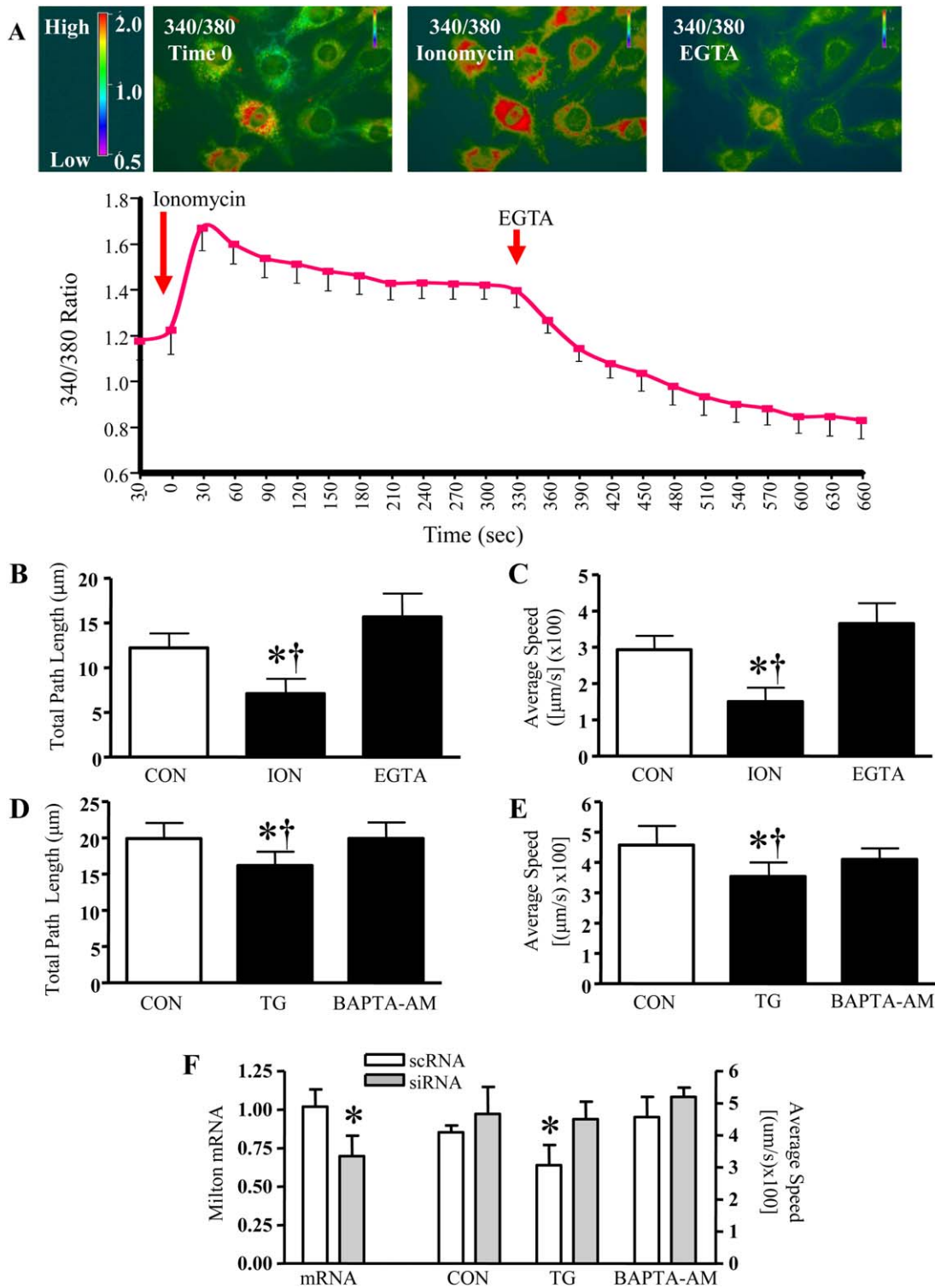
Fig. 4. **Cytosolic calcium regulates mitochondrial movement in myoblasts. A**: Intracellular calcium levels were assessed in Fura2-AM loaded C_2C_{12} cells. Fura2 fluorescence was measured using excitation of Ca^{2+}-bound (340 nm, red) and the Ca^{2+}-free form (380 nm, green). Thus, elevations evoked by the addition of Ionomycin (ION) and Thapsigargin (TG) appear as increases in the red component. Elevated calcium concentrations were achieved through the addition of ionomycin and reduced by EGTA. **B, C**: Increased calcium attenuated mitochondrial movement, and organelle transport was recovered by the addition of EGTA. Endogenous calcium levels were elevated with Thapsigargin treatment and suppressed with BAPTA-AM. **D, E**: High calcium concentrations inhibited the total path length and the average velocity traveled by the organelles. ($n = 6$–8, *$P < 0.05$ vs CON). **F**: Milton mRNA levels were assessed in myoblasts treated with 100 nM of scRNA or siRNA specific for Milton (left). The average speed traveled by mitochondria was determined in scRNA and siRNA transfected C_2C_{12} cells, treated with Thapsigargin and BAPTA-AM (right).

average speed, and (3) percentage of time that organelles remained stationary. Our results indicate that microtubule disruption resulted in greater impediments in mitochondrial motility as compared to conditions in which actin polymerization was disturbed in myoblasts. Administration of microtubule depolymerizing or stabilizing agents resulted in similar effects on mitochondrial motility, yet they varied in the degree of their effects. The presence of taxol enhanced the stability of microtubules, rendering them more susceptible to undergoing post-translational modifications, such as acetylation, detyrosination, and polyglutamylation [Hammond et al., 2010]. These post-translational modifications may explain the disparity between the effects of taxol and nocodazole or colchicine treatments

Since kinesin and dynein motors drive the movement of mitochondria along microtubules, we speculated that the downregulation of these components would alter organelle transport. By reducing the levels of Kif5B, a member of the Kinesin-1 family, we observed decreased mitochondrial motility. It has previously been reported that the deletion of similar kinesin-1 family members in fungus and mouse neurons, led to altered mitochondrial distribution [Tanaka et al., 1998; Wu et al., 1998]. Analyses in the Drosophila nervous system support the concept that the primary motors for mitochondrial movement are Kinesin-1, in coordination with dynein, which moves mitochondria in the opposite direction [Pilling, 2006].

Calcium influx has been found to inhibit mitochondrial movement in neurons and cardiac myocytes using motor protein/adapter complexes [Yi et al., 2004; Wang and Schwarz 2009]. However, the influences of Ca^{2+} within skeletal muscle, as well as the mechanism by which Ca^{2+} exerts its effects are still under investigation. Our results indicate that elevations in Ca^{2+} exert a negative effect on mitochondrial movement, and cause an inhibition of motility. Linker proteins coordinate the movement of mitochondria with environmental signals, and are necessary for proper localization of the organelle. In neurons, HEK293 and COS-7 cells, Milton acts as a mitochondrial-specific linker that redistributes the organelle to appropriate regions within the cell, in response to increases in Ca^{2+} [Stowers et al., 2002; Smith et al., 2006; Wang and Schwarz, 2009]. Mutations in the protein result in mitochondrial trafficking defects, while other organelles retain their normal distribution [Stowers et al., 2002]. In this context, it is interesting that we observed Milton to also have a vital role in mitochondrial movement when Ca^{2+} levels were elevated in myoblast cells. Inhibition of Milton disrupted Ca^{2+}-induced mitochondrial transport. Thus, Milton may mediate associations between Kinesin-1 and mitochondria in muscle cells.

We next wanted to examine the effect that chronic changes in motility might have on mitochondrial content. Argyropoulos et al. previously found that inhibition of the motor protein, Kif5B, reduced cytochrome b mRNA [Argyropoulos et al., 2009]. Therefore, we speculated that reductions in Kif5B would alter the expression of proteins involved in mitochondrial biogenesis. We observed no change when we examined the prominent regulator of mitochondrial biogenesis, PGC-1α, as well as the mitochondrially- and nuclear-encoded proteins COXI and COXIV, respectively. Therefore, our data are not consistent with a role for changes in motor protein expression on mitochondrial biogenesis.

In summary, mitochondria primarily move along microtubules tracks. In myoblasts, mitochondria can pause, change their direction, and their velocity of movement. We demonstrated that organelle displacement within myoblasts is regulated by Ca^{2+} signals, which inhibit mitochondrial movements in a Milton-dependent manner. By understanding mitochondrial movements and the signaling events that regulate their dynamics, we can elucidate the underlying basis for organelle interactions, leading to the formation of the mitochondrial reticulum and the distribution of energy in muscle cells.

Materials and Methods

Overview of the Experimental Strategy

To elucidate which cytoskeletal component is primarily responsible for mitochondrial movement within myoblasts, we initially began by using a pharmacological approach to disrupt actin and microtubules. Subsequently, we sought to establish which motor proteins were involved in mitochondrial dynamics by using siRNA technology. Finally, since calcium is an important regulator of mitochondrial function, we sought to determine the relationship between mitochondrial motility and calcium signaling in myoblasts.

Cell Culture and Transfections

C_2C_{12} murine skeletal muscle cells were grown in DMEM supplemented with 10% fetal bovine serum and 1% Penicillin/Streptomycin (Growth Media, GM). Cells were cultured in custom made glass bottom culture plates and maintained at 37°C in 5% CO_2. Upon reaching a confluence of approximately 60%, mito-DsRED2 was transfected into myoblasts using Lipofectamine 2000 (Life Technologies) to visualize mitochondria. Mitochondrial movement was observed in C_2C_{12} cells using an expression vector that encodes a fusion of red fluorescence protein and the mitochondrial targeting sequence from cytochrome c oxidase subunit VIII (mito-dsRED2).

Treatments

Forty-eight hours following transfection with mito-DsRed2, myoblasts were treated with microtubule and/or actin disrupting drugs, or a vehicle control (DMSO; Sigma-Aldrich). Microtubules were depolymerized using nocodazole (20μM; Toronto Research Chemicals) and colchicine (20 μM; Sigma-Aldrich), while Taxol (2 μM; Sigma-Aldrich) was used for stabilization. Actin was

disrupted using cytochalasin D (2 µM; Enzo Life Sciences). Pre-incubation with these agents was 1 hr prior to imaging.

In order to study the regulation of mitochondrial dynamics by calcium, C_2C_{12} cells were treated with either ionomycin (1 µM, Sigma-Aldrich), a Ca^{2+} ionophore, or thapsigargin (1 µM, Enzo Life Science), an inhibitor of the sarcoplasmic reticulum Ca^{2+}-ATPase. Ca^{2+} levels were suppressed using the chelators EGTA (5 mM, Sigma-Aldrich) and BAPTA-AM (2 µM, Calbiochem).

Mitochondrial Movement Analysis

Mitochondria were visualized using an inverted Nikon Eclipse TE2000-U fluorescent microscope equipped with 100×/1.5 oil objective lens, with a custom designed chamber designed to maintain a constant temperature of 37°C with 5% CO_2. Mitochondrial dynamics were captured at 2 sec intervals for a total time of 5 mins using real-time imaging. Analyses were performed using the NIS Element AR 3.1 software, and was limited to regions of interest in the periphery of the cells, where individual mitochondria were readily resolved and could be used for analysis, while avoiding the confounding influence of high density mitochondrial networks.

Immunocytochemistry of Actin and Microtubules

For immunocytochemistry, the transfected cells were washed 3× with PBS at room temperature. The cells were then fixed with 3.7% formaldehyde for 7 min and washed with 3× with PBS. Cells were permeabilized with 0.1% Triton X-100 at 4°C for 15 min and washed 3× with PBS. Subsequently, cells were stained with a FITC conjugated α-tubulin primary antibody (Abcam), or Acti-stain 488 phalloidin (Cytoskeleton Inc) for 2 hrs or 30 mins, respectively. The cells were then washed 3× with PBS and incubated with DAPI (Sigma-Aldrich) for 5 mins to stain the DNA. After washing twice with PBS, the media was replaced with GM without phenol red.

RNA Interference

Silencer Select predesigned small interfering RNA (siRNA) for Kif5B (5′-GACAUGUCGCAGUUACAATT-3′), dynein (Dynch1; 5′-GAAAGAUCCGCAACACGAATT-3′), Milton (TRAK1; 5′-GCAACGUGGUCCUCGAUAATT-3′) and scrambled controls (scRNA) were used in the knockdown experiments (Ambion). To produce knockdowns, the media was switched to pre-transfection media (DMEM and 10% FBS). The following day, the media was changed to DMEM and myoblasts were incubated with mito-DsRED2, and either 50 nM of siRNA specific for Kif5B or dynein, or 100 nM of siRNA for TRAK1, along with 10 µl of Lipofectamine 2000 for 6 hrs. Concomitantly, scrambled nontargeting siRNA underwent the same conditions. Forty-eight hours post-transfection, cells were used for image analysis or were collected for protein extracts.

Immunoblotting

Protein extracts from myoblasts were separated on 6–15% SDS-PAGE and subsequently transferred onto nitrocellulose membranes. Membranes were then blocked (1 hr or 1.5 hr) with a 5% skim milk in 1× TBS-Tween20 solution (Tris-buffered saline–Tween-20: 25 mM Tris–HCl, pH 7.5, 1 mM NaCl and 0.1% Tween-20) at room temperature, followed by incubation in blocking solution with antibodies directed towards Kif5B (1:500; Santa Cruz), Dynein heavy chain (1:1000; Santa Cruz), PGC-1α (1:500; Millipore), COX IV (1:250; Abcam), COX I (1:500; MitoSciences), or α-tubulin (1:2000; Calbiochem) overnight at 4°C. Subsequently, membranes were washed 3× 5 min with TBS-Tween20, followed by incubation at room temperature (1 hr) with the appropriate secondary antibody conjugated to horseradish peroxidase, and washed again 3× for 5 min each with TBS-Tween20. Membranes were developed using Western Blot Luminol Reagent (Santa Cruz). Films were subsequently scanned and quantified via densitometric analysis for the intensity of signals with SigmaScanPro software (version 5, Jandel Scientific).

Real-Time PCR

Total RNA was extracted from C_2C_{12} cells 48 hrs after transfection, as previously described (Ostojic et al., 2013). The concentration and purity of the RNA was assessed using absorbance readings at 260 and 280 nm (Ultrospec 2100 Pro). In accordance with the manufacturer's recommendations, SuperScript® III reverse transcriptase (Invitrogen) was used to reverse transcribe the RNA into cDNA. Using sequences from GenBank, primers were designed with Primer 3 v. 0.4.0 software (Massachusetts Institute of Technology, Cambridge, MA) for Milton as the gene of interest, with glyceraldehyde-3-phosphate dehydrogenase (GAPDH) and β2-microglobulin (β2M) serving as the endogenous controls. The primers used were as follows: Milton forward: 5′-GGGAACGAGGACCACAATAA-3′, Milton reverse: 5′-CCTCCGCTCAGACAGGTAGT-3′, GAPDH forward: 5′-AACACTGAGCATCTCCCTCA-3′, GAPDH reverse: 5′-GTGGGTGCAGCGAACTTTAT-3′, β2M forward: 5′-GGTCTTTCTGGTGCTTGTCT-3′, β2M reverse: 5′-TATGTTCGGCTTCCCATTCT-3′. Quantification of the gene of interest was corrected using the endogenous controls and analyzed as previously described (Ostojic et al., 2013).

Oxygen Consumption

Oxygen consumption was determined based on fluorescence quenching by oxygen using OxoPlates (Innovative Instruments). Cells were added to each well at a density of 8000 cells/well. The following day, cells were pre-incubated (1 hr) with the microtubules and/or actin disrupting agents. Optical oxygen sensors at the bottom of microplates contained an indicator and a reference dye. Wells containing air-saturated (100%) and oxygen-free (0%) solutions were

used for calibration. Fluorescence was assessed for 3.5 hrs in 3 min intervals in dual kinetic mode (Synergy HT microplate reader), using filter 1 (530/645 nm) and filter 2 (530/590) settings in order to detect fluorescence of the indicator and reference dyes, respectively. From these values, ratios were calculated and compared to the standard calibrations, thus allowing quantification of oxygen consumption.

Calcium Imaging

Cells were washed with GM without phenol red and incubated in the dark for 40 mins in a solution containing the calcium-sensitive dye fura-2-acetoxymethyl ester (Fura-2 AM, 5 μM) and 0.02% pluronic F-127. Fura-2 AM-loaded cells were washed twice and the media was replaced with GM without phenol red for an additional 20 mins to allow the de-esterification of fura-2 AM to occur. Prior to imaging, the media was replaced. Ratiometric imaging at absorption wavelengths of 340 and 380 nm (emission 510 nm) was taken at 30 sec intervals. Changes in the ratio of fluorescence intensity obtained at 340 nm (fura-2-Ca^{2+} bound) to that of 380 nm (Ca^{2+} free fura-2) were used to assess Ca^{2+} levels following the addition of either ionomycin or thapsigargin to the media, to stimulate the release of calcium, and following the chelation of calcium by EGTA or BAPTA-AM.

Statistical Analyses

Data were analyzed with GraphPad 4.0 software and expressed as means ± SE. *T*-tests and one-way ANOVAs were performed where appropriate, and differences were considered statistically significant if $P < 0.05$.

References

Aizawa H, Sekine Y, Takemura R, Zhang Z, Nangaku M, Hirokawa N. 1992. Kinesin family in murine central nervous system. J Cell Biol 119;1287–1296.

Argyropoulos G, Stutz A M, Ilnytska O, Rice T, Teran-Garcia M, Rao D C, Bouchard C, Rankinen T. 2009. KIF5B gene sequence variation and response of cardiac stroke volume to regular exercise. Physiol Genomics 36;79–88.

Bindokas VP, Lee CC, Colmers WF, Miller RJ. 1998. Changes in mitochondrial function resulting from synaptic activity in the rat hippocampal slice. J Neurosci 18;4570–4587.

Crompton M, Costi A. 1988. Kinetic evidence for a heart mitochondrial pore activated by Ca2+, inorganic phosphate and oxidative stress. A potential mechanism for mitochondrial dysfunction during cellular Ca2+ overload. Eur J Biochem 178;489–501.

De Vos KJ, Allan VJ, Grierson AJ, Sheetz MP. 2005. Mitochondrial function and actin regulate dynamin-related protein 1-dependent mitochondrial fission. Curr Biol 15;678–683.

Fabricius C, Berthold CH, Rydmark M. 1993. Axoplasmic organelles at nodes of Ranvier. II. Occurrence and distribution in large myelinated spinal cord axons of the adult cat. J Neurocytol 22;941–954.

Glater EE, Megeath LJ, Stowers RS, Schwarz TL. 2006. Axonal transport of mitochondria requires milton to recruit kinesin heavy chain and is light chain independent. J Cell Biol 173;545–557.

Hammond JW, Huang CF, Kaech S, Jacobson C, Banker G, Verhey KJ. 2010. Posttranslational modifications of tubulin and the polarized transport of kinesin-1 in neurons. Mol Biol Cell 21;572–583.

Hirokawa N, Noda Y, Tanaka Y, Niwa S. 2009. Kinesin superfamily motor proteins and intracellular transport. Nat Rev Mol Cell Biol 10;682–696.

King SR, Stocco DM. 1996. ATP and a mitochondrial electrochemical gradient are required for functional activity of the steroidogenic acute regulatory (StAR) protein in isolated mitochondria. Endocr Res 22;505–514.

Macaskill AF, Rinholm JE, Twelvetrees AE, rancibia-Carcamo IL, Muir J, Fransson A, Aspenstrom P, Attwell D, Kittler JT. 2009. Miro1 is a calcium sensor for glutamate receptor-dependent localization of mitochondria at synapses. Neuron 61;541–555.

Mitchison T, Kirschner M. 1984. Dynamic instability of microtubule growth. Nature 312;237–242.

Morris RL, Hollenbeck PJ 1993 The regulation of bidirectional mitochondrial transport is coordinated with axonal outgrowth. J Cell Sci 104;917–927.

Morris RL, Hollenbeck PJ 1995 Axonal transport of mitochondria along microtubules and F-actin in living vertebrate neurons. J. Cell Biol 131;1315–1326.

Nangaku M, Sato-Yoshitake R, Okada Y, Noda Y, Takemura R, Yamazaki H, Hirokawa N. 1994. KIF1B, a novel microtubule plus end-directed monomeric motor protein for transport of mitochondria. Cell 79;1209–1220.

Nguyen PV, Marin L, Atwood HL. 1997. Synaptic physiology and mitochondrial function in crayfish tonic and phasic motor neurons. J Neurophysiol 78;281–294.

Ostojic O, O'Leary MF, Singh K, Menzies KJ, Vainshtein A, Hood DA. 2013. The effects of chronic muscle use and disuse on cardiolipin metabolism. J Appl Physiol (1985) 114;444–452.

Pilling AD, Horiuchi D, Lively CM, Saxton WM. 2006. Kinesin-1 and Dynein are the primary motors for fast transport of mitochondria in Drosophila motor axons. Mol Biol Cell 17;2057–2068.

Saotome M, Safiulina D, Szabadkai G, Das S, Fransson A, Aspenstrom P, Rizzuto R, Hajnoczky G. 2008. Bidirectional Ca2+-dependent control of mitochondrial dynamics by the Miro GTPase. Proc Natl Acad Sci USA 105;20728–20733.

Simon VR, Karmon SL, Pon LA. 1997. Mitochondrial inheritance: cell cycle and actin cable dependence of polarized mitochondrial movements in *Saccharomyces cerevisiae*. Cell Motil Cytoskeleton 37;199–210.

Smith MJ, Pozo K, Brickley K, Stephenson FA. 2006. Mapping the GRIF-1 binding domain of the kinesin, KIF5C, substantiates a role for GRIF-1 as an adaptor protein in the anterograde trafficking of cargoes. J Biol Chem 281;27216–27228.

Stowers RS, Megeath LJ, Gorska-Andrzejak J, Meinertzhagen IA, Schwarz TL. 2002. Axonal transport of mitochondria to synapses depends on milton, a novel Drosophila protein. Neuron 36;1063–1077.

Tanaka Y, Kanai Y, Okada Y, Nonaka S, Takeda S, Harada A, Hirokawa N. 1998. Targeted disruption of mouse conventional kinesin heavy chain, kif5B, results in abnormal perinuclear clustering of mitochondria. Cell 93;1147–1158.

Wang X, Schwarz TL. 2009. The mechanism of Ca2+ -dependent regulation of kinesin-mediated mitochondrial motility. Cell 136;163–174.

Wu Q, Sandrock TM, Turgeon BG, Yoder OC, Wirsel SG, Aist JR. 1998. A fungal kinesin required for organelle motility, hyphal growth, and morphogenesis. Mol Biol Cell 9;89–101.

Yi M, Weaver D, Hajnoczky G. 2004. Control of mitochondrial motility and distribution by the calcium signal: a homeostatic circuit. J Cell Biol 167;661–672.